

# Reducing adhesion energy of nano-electro-mechanical relay contacts by self-assembled Perfluoro (2,3-Dimethylbutan-2-ol) coating

Cite as: AIP Advances 9, 055329 (2019); <https://doi.org/10.1063/1.5095760>

Submitted: 12 March 2019 . Accepted: 20 May 2019 . Published Online: 30 May 2019

Sara Fathipour, Sergio Fabian Almeida, Zhixin Alice Ye, Bivas Saha, Farnaz Niroui, Tsu-Jae King Liu, and Junqiao Wu



View Online



Export Citation



CrossMark

AVS Quantum Science

Co-published with AIP Publishing



Coming Soon!

# Reducing adhesion energy of nano-electro-mechanical relay contacts by self-assembled Perfluoro (2,3-Dimethylbutan-2-ol) coating

Cite as: AIP Advances 9, 055329 (2019); doi: 10.1063/1.5095760

Submitted: 12 March 2019 • Accepted: 20 May 2019 •

Published Online: 30 May 2019



View Online



Export Citation



CrossMark

Sara Fathipour,<sup>1,a)</sup> Sergio Fabian Almeida,<sup>2</sup> Zhixin Alice Ye,<sup>2</sup> Bivas Saha,<sup>1,3</sup> Farnaz Niroui,<sup>4</sup> Tsu-Jae King Liu,<sup>2</sup> and Junqiao Wu<sup>1,3,b)</sup>

## AFFILIATIONS

<sup>1</sup>Department of Materials Science and Engineering, University of California, Berkeley, California 94720, USA

<sup>2</sup>Department of Electrical Engineering and Computer Sciences, University of California, Berkeley, California 94720, USA

<sup>3</sup>Materials Sciences Division, Lawrence Berkeley National Laboratory, Berkeley, California 94720, USA

<sup>4</sup>Department of Electrical Engineering and Computer Science, Massachusetts Institute of Technology, Cambridge, Massachusetts 02139, USA

<sup>a)</sup>Electronic email: [sarafathipour3@berkeley.edu](mailto:sarafathipour3@berkeley.edu)

<sup>b)</sup>Electronic email: [wuj@berkeley.edu](mailto:wuj@berkeley.edu)

## ABSTRACT

To enable energy-efficient electronic devices for the future, nano-electro-mechanical (NEM) relays are promising due to their high ON/OFF current ratio and potential for low operating voltage. To minimize hysteresis and, consequently, relay operating voltage, it is imperative to reduce the relay contact adhesion, which can be achieved by coating the contacts with anti-stiction self-assembled monolayers. Herein we report a 71% reduction in hysteresis voltage by utilizing a branched perfluorocarbon antistiction molecule: Perfluoro (2,3-Dimethylbutan-2-ol) (PDB) on top of the tungsten contact surfaces. Experimental results show the operation of a PDB-coated NEM relay with abrupt switching, undetectably low OFF-state current, hysteresis voltage as low as 20 mV, and a large ON/OFF current ratio ( $>10^7$ ).

© 2019 Author(s). All article content, except where otherwise noted, is licensed under a Creative Commons Attribution (CC BY) license (<http://creativecommons.org/licenses/by/4.0/>). <https://doi.org/10.1063/1.5095760>

Reducing supply voltage, while keeping OFF-state leakage current low is essential for reducing energy consumption in electronic devices. To keep the ON-state performance of a metal-oxide-semiconductor field effect transistor (MOSFET), it is desired to reduce the threshold voltage along with the supply voltage. However, reducing threshold voltage in a MOSFET results in an exponential increase in the OFF-state leakage current. This constraint is unavoidable in a MOSFET, because the subthreshold swing cannot be reduced below 60 mV/decade at 300 K.<sup>1–3</sup> On the other hand, nano-electro-mechanical switches (NEMs) have a steep switching slope with undetectably low OFF-state leakage current and therefore are of keen interest for ultra-low power applications and mobile battery-powered electronic devices.<sup>4,5</sup> NEMs use a gate voltage to

make or break a contact between source and drain electrodes, and as such, contact adhesion is a critical factor in determining the energy efficiency of NEM switches.<sup>6,7</sup> Contact adhesion leads to hysteresis in switching and limits the scaling of the operating voltage.<sup>8</sup> Therefore, reducing contact adhesion is critical to achieving energy efficient NEM relays.

Previously, it has been shown that fluorinated self-assembled molecular coatings can be integrated into prefabricated NEM relays to reduce contact adhesion and hysteresis voltage.<sup>9,10</sup> In particular, 1H,1H,2H,2H-perfluorodecyltriethoxysilane (PFDTES)<sup>11,12</sup> and perfluorooctyltriethoxysilane (PFOTES)<sup>12,13</sup> self-assembled molecular layers have been explored as anti-stiction coatings for NEM relays. The relays coated with these self-assembled molecular

layers have shown low hysteresis voltage stability over 100 gate voltage sweeps<sup>12</sup> and a turn on delay of 1.5  $\mu\text{s}$  with 50 mV operation voltage.<sup>13</sup> The silane functional head group in these molecules facilitates self-assembly onto the contacting electrodes, while their fluorinated spacer group and a  $\text{CF}_3$  terminal group help to reduce surface adhesion energy. PFDTES and PFOTES self-assembled molecules have seven and five difluoromethane ( $\text{CF}_2$ ) in their backbone chain and are  $\sim 1.5$  nm and  $\sim 1.3$  nm long, respectively. The ability of perfluorinated carbon chains to reduce adhesion lies in their low polarizability at the molecular scale, since the interaction energy arising from London forces varies as the square root of polarizability.<sup>14</sup> As the molecule is progressively fluorinated, the dipole moment of the terminal  $\text{CF}_3$  group can be distributed throughout the molecule.<sup>15</sup> Therefore, longer single chain self-assembled molecules with more difluoromethanes in their backbone are more effective in reducing adhesion (Figure 1(a)). However, reducing adhesion by inserting more difluoromethanes in the backbone chain of self-assembled molecules happens at the expense of degrading the ON-state conduction and switching slope of a NEM relay. This is due to the insulating nature of self-assembled molecules.

To alleviate the trade-off between switching slope and adhesion force, perfluoro (2,3-dimethylbutan-2-ol) (PDB), which is a branched self-assembled molecule, was used in this work. The length of PDB is  $\sim 0.5$  nm, a factor of three shorter than PFDTES and PFDTES. The branched nature of this molecule provides enough fluorine atoms to reduce adhesion without the need to increase the length of the molecule by adding difluoromethanes in the backbone chain. This is shown schematically in Figure 1(b). Since the molecule can be kept short, the switching slope of the coated relay will not be substantially degraded while surface adhesion is drastically reduced.

The chemical structure of PDB is shown in Figure 1(c). The hydroxyl head group of PDB facilitates self-assembly on the NEM relay's tungsten electrodes. The mechanism for self-assembly of PDB on tungsten electrodes through the hydroxyl head group is shown schematically in Figure S1 of the supplementary material.

To characterize the PDB coating, PDB was grown on a silicon wafer coated with 60 nm of tungsten, using a vapor-phase self-assembly process. A few droplets of PDB were placed in close proximity to the wafer in a desiccator. The pressure in the desiccator was then reduced to 1 Torr using a vacuum pump. The wafer was left in the desiccator for 8 hours to complete the assembly process.

In order to confirm successful assembly of PDB on the wafer, x-ray photoelectron spectroscopy (XPS) was performed. Figure 2(a) shows the XPS spectra of tungsten coated silicon wafer before and after the PDB growth. A clear fluorine peak detected on the functionalized sample suggests successful assembly of PDB on tungsten surface. As a point of reference, XPS survey of the wafer before the PDB growth displays no fluorine peak.

Atomic force microscopy (AFM) was previously used in the force spectroscopic mode to determine the dependence of probe-sample interaction on the distance between the probe tip and the sample.<sup>16–18</sup> Figure S2 in the supplementary material shows a typical force-displacement curve in atomic force microscopy along with the corresponding vertical tip movement as it approaches and retracts away from the surface. Here, we use this technique to measure the adhesive force between the AFM tip and the tungsten coated silicon wafer after the PDB assembly. A microspherical  $\text{SiO}_2$  tip with a tip diameter of  $2 \mu\text{m}$  was used in the AFM measurements, as the conventional sharp AFM tips do not yield consistent results.<sup>19</sup> Measurements were done in  $\text{N}_2$  to eliminate the contribution of capillary forces due to the presence of water molecules.<sup>20</sup>

The adhesion energy can be calculated from the measured adhesive force between a flat surface and a sphere using Derjaguin-Muller-Toporov (DMT) theory:<sup>21</sup>

$$W_{ad} = \frac{F_{ad}}{2\pi r}, \quad (1)$$

where  $W_{ad}$  is the adhesion energy per unit area,  $F_{ad}$  is the measured adhesive force, and  $r$  is the radius of the AFM tip. Figure 2(b) compares the calculated value of adhesion energy for PDB coating with those of trimethoxy(3,3,3-trifluoropropyl) silane (PFTTES) and the coatings used in the prior reports, PFDTES<sup>11,12</sup> and PFOTES.<sup>12,13</sup>

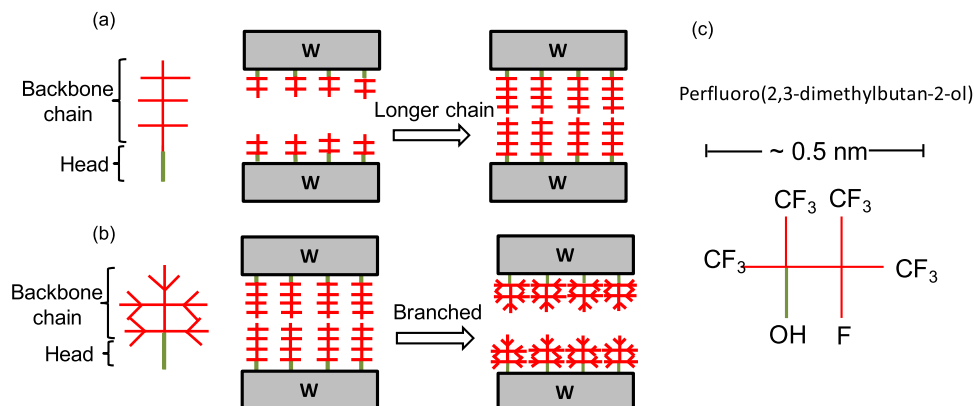


**FIG. 1.** Schematic of (a) single-chain and (b) branched self-assembled molecular coating. Green and red colors show head functional group and backbone of the molecule, respectively. To further reduce the adhesive force, more  $\text{CF}_2$  groups can be inserted into the backbone of the molecule as in (a). However, making the backbone longer deteriorates the on-state conduction and switching slope of the NEM relay. Alternatively, branched self-assembled molecular coatings can be used as in (b) that are shorter and therefore do not affect the on-state conduction significantly. (c) Chemical structure schematic of PDB, the branched molecule used in this work.

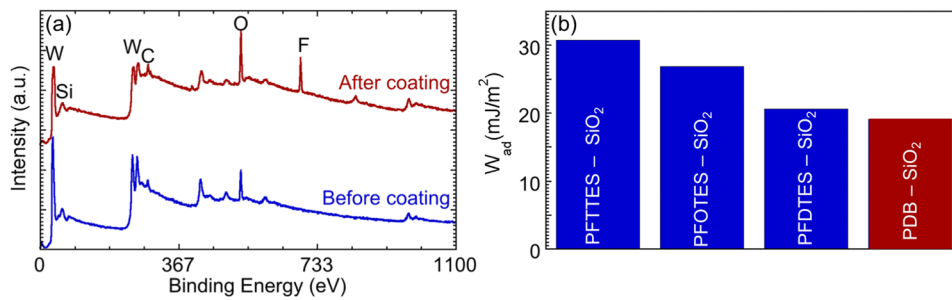


**FIG. 2.** (a) X-ray photoelectron spectra (XPS) of tungsten coated silicon wafer before and after PDB assembly, confirming successful surface fluorination. For better visualization, the spectra of before and after coating are offset with respect to each other. (b) Values of adhesion energy per unit area between PFTTES, PFOTES, PFDTES, PDB and SiO<sub>2</sub> tip measured with AFM in the force spectroscopic mode.

Similar to PFDTES and PFOTES, PFTTES has a silane functional head group to promote its self-assembly onto tungsten, but it does not have any difluoromethanes in its backbone chain. As can be deduced from Figure 2(b), the adhesion energy between SiO<sub>2</sub> tip and PDB is the smallest compared to the other molecular layers considered here.

Once successful PDB assembly on tungsten surface was confirmed with XPS, the molecular coating was incorporated into pre-fabricated NEM relays. Figure 3(a) shows the scanning electron microscope (SEM) image of the four-terminal NEM relay used in this work. The NEM relay comprises a movable gate electrode suspended by four folded-flexure beams over a fixed body electrode, and source/drain electrodes, as shown in Figure 3(b). By designing a relatively stiff structure (spring constant  $\sim 700$  N/m), we can avoid the probability of the device turning on without applying any voltage or its structural collapse. The source is attached to the gate electrode but electrically isolated by an intermediary oxide film. In contrast to the six-terminal NEM relays presented in Ref. 13, this design has four terminals: body, gate, and a single source and drain. The single contact design is used to enable study of the effect of adhesion energy on a single contact area. The source contacts the drain at the center of the movable electrode. When a sufficiently large voltage (pull-in voltage,  $V_{PI}$ ) is applied across the gate and the body, which can be considered as two plates of a parallel plate capacitor, the resultant electrostatic force displaces the gate electrode towards the body electrode, causing the source and the drain electrodes to come into contact, as shown in Figure 3(c).

The electrostatic force between the gate and the body is balanced by the spring restoring force of the deformed suspension beams. Applying an excessive voltage between the gate and the body, much larger than  $V_{PI}$ , can collapse the structure and cause a catastrophic failure. The separation between source and drain occurs when the gate voltage,  $V_{GS}$ , reaches the release voltage,  $V_{RL}$  (which is smaller than  $V_{PI}$ ), and the spring restoring force from the folded flexures of the movable electrodes is able to overcome the source-drain contact adhesive force. Therefore, these devices exhibit a hysteresis in operation, characterized by a hysteresis voltage, which is the difference between the pull-in and the release voltages. In order to guarantee low hysteresis, the ratio between the contact and actuation gaps ( $g_d$  and  $g_o$  in Figure 3(b)) for the NEM relays used in this study is designed to be smaller than 1/3.<sup>22</sup> Therefore, the difference between the pull-in and the release voltages is only due to the adhesion force between the source and the drain contacts and there is no inherent hysteresis in the operation of these devices as in pull-in mode relays. The fabrication process flow for the relay used in this study is discussed in detail in the [supplementary material](#). The cross-sectional views along AA', BB' and CC' cutlines in Figure 3(a) are shown in Figure S3(a) for each step in the fabrication flow.

The relays in this work were tested at room temperature in a vacuum probe station to avoid oxidation of the tungsten electrodes, which can otherwise degrade the contact resistance. Figure 4(a) shows the transfer characteristics of the NEM relay before and after implementing a PDB coating and without body biasing. The ON current is limited to 10  $\mu$ A by the current compliance

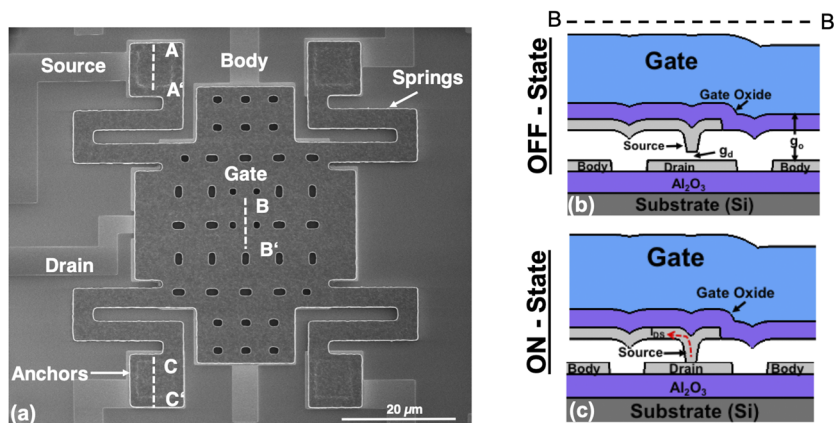


**FIG. 3.** (a) SEM image of the four-terminal relay used in this work. The BB' cross section for (b) the OFF-state and (c) ON state of the device. In the OFF state, a 60 nm airgap separates source and drain electrodes and therefore the OFF-state leakage current is undetectably low. In the ON state of the device, the electrostatic force between the gate and the body electrodes brings the source and the drain into contact, allowing an abrupt increase in current conduction.

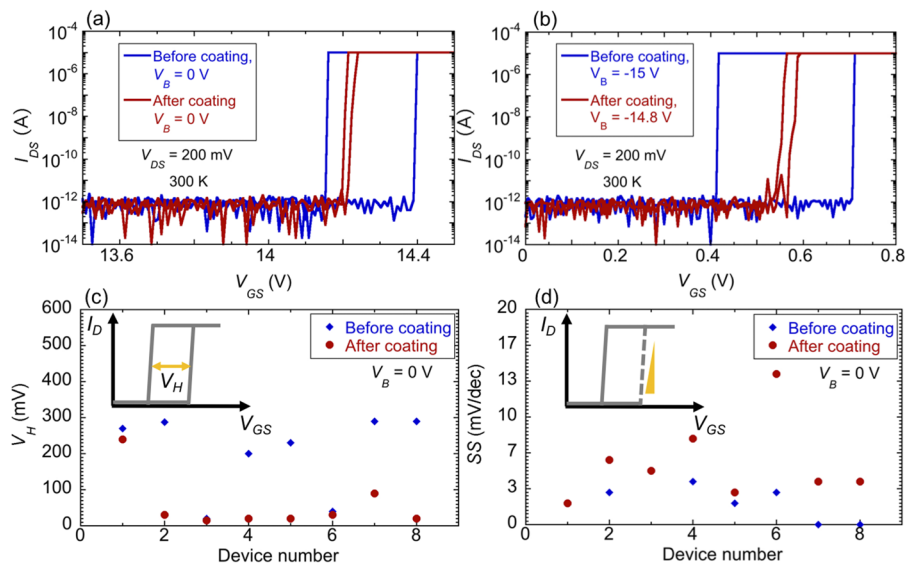


**FIG. 4.** Measured  $I$ - $V$  characteristics for NEM relays before and after PDB coating (a) without body-bias and (b) with body-bias. Measured (c) hysteresis voltages and (d) switching slopes for multiple relays before and after PDB coating.

set by the measurement equipment (Agilent B1500A Device Analyzer). The hysteresis voltage ( $V_H$ ) was substantially reduced from  $\sim 240$  mV before coating to  $\sim 20$  mV after PDB coating, while the switching slope was not significantly affected. The relay in Figure 4(a) is operating at a gate voltage range of up to  $\sim 14.5$  V. To avoid increasing the switching energy and to reduce the gate voltage swing that is required for operating the relay, pull-in voltage can be tuned by adjusting the body bias ( $V_B$ ) as shown in Figure 4(b).<sup>22</sup>

The effect of PDB coating on hysteresis voltage of eight measured NEM relays is shown in Figure 4(c). The average hysteresis voltage was decreased from 204 mV before coating to 58 mV after coating, displaying the significant contribution that the molecular coating can have in reducing the operating voltage of a NEM relay. This reduction in the hysteresis voltage is achieved without any adverse effects on the switching slope as can be seen in Figure 4(d).

In conclusion, we have used a branched self-assembled molecular coating, PDB ( $\sim 0.5$  nm long), to reduce adhesion and thereby hysteresis voltage in a NEM relay. The reduction of hysteresis voltage is crucial for minimizing the operating voltage in NEM relay-based circuits. The branched nature of PDB backbone provides enough fluorine atoms for reducing adhesion without degrading the electrical conduction as the molecule's length can remain sufficiently small. An average reduction of 71% was achieved in hysteresis voltage of the relays after PDB coating, while the switching slope was not significantly affected.

See [supplementary material](#) for the mechanism of PDB self-assembly on tungsten surface, adhesive force measurement with AFM and the process flow for the NEM relay used in this work.

The work was supported by the Center for Energy Efficient Electronics Science (NSF Award No. 0939514). The NEM relays were fabricated in the Marvell Nanofabrication Laboratory and XPS experiments were performed at the Biomolecular Nanotechnology

Center at the University of California at Berkeley, Berkeley, CA, USA.

The authors declare no conflicts of interest.

## REFERENCES

- S. Hanson, B. Zhai, K. Bernstein, D. Blaauw, A. Bryant, L. Chang, K. K. Das, W. Haensch, E. J. Nowak, and D. M. Sylvester, *IBM J. Res. Develop* **50**(4.5), 469–490 (2006).
- T. Skotnicki, J. A. Hutchby, T.-J. K. Liu, H.-S. P. Wong, and F. Boeuf, *IEEE Circuits Dev. Mag.* **21**(1), 16–26 (2005).
- A. M. Ionescu and H. Riel, *Nature* **479**(7373), 329–337 (2011).
- V. Pott, H. Kam, R. Nathanael, J. Jeon, E. Alon, and T.-J. K. Liu, *Proc. IEEE* **98**(12), 2076–2094 (2010).
- M. Spencer, F. Chen, C. C. Wang, R. Nathanael, H. Fariborzi, A. Gupta, H. Kam, V. Pott, J. Jeon, T.-J. K. Liu, D. Markovic, E. Alon, and V. Stojanovic, *IEEE J. Solid-State Circuits* **46**(1), 308–320 (2011).
- J. Young, L. Hutin, J. Jeon, and T.-J. K. Liu, *J. Microelectromech. Syst.* **23**(1), 198–203 (2014).
- B. Jensen, K. Huang, L. L. W. Chow, and K. Kurabayashi, *J. Appl. Phys.* **97**(10), 103535 (2005).
- C. Pawashe, K. Lin, and K. J. Kuhn, *IEEE Trans. Elec. Dev.* **60**(9), 2936–2942 (2013).
- F. Niroui, J. Patil, T. Swager, J. Lang, and V. Bulović, 2017 Fifth Berkeley Symp. Energy Efficient Electronic Syst. & Steep Transistors Workshop (E3S), 1–3.
- R. Maboudian, W. R. Ashurst, and C. Carraro, *Sens. Actuators* **82**, 219–223 (2000).
- B. Osoba, B. Saha, L. Dougherty, J. Edgington, C. Qian, F. Niroui, J. H. Lang, V. Bulović, J. Wu, and T.-J. K. Liu, 2016 Int. Electron Dev. Meeting (IEDM), 655–658.
- B. Osoba, B. Saha, S. F. Almeida, J. Patil, L. E. Brandt, M. E. D. Roots, E. Acosta, J. Wu, and T.-J. K. Liu, *IEEE Trans. Electron Dev.* **65**(4), 1529–1534 (2018).
- Z. A. Ye, S. Almeida, M. Rusch, A. Perlas, W. Zhang, U. Sikder, J. Jeon, V. Stojanović, and T.-J. K. Liu, 2018 Int. Electron Dev. Meeting (IEDM), 4.1.1–4.1.4.
- D. M. Lemal, *J. Organic Chem.* **69**(1), 1–11 (2004).

- <sup>15</sup>N. L. Jarvis and W. A. Zisman, *J. Phys. Chem.* **63**, 727 (1959).
- <sup>16</sup>A. L. Weisenhorn, P. K. Hansma, T. R. Albrecht, and C. F. Quate, *Appl. Phys. Lett.* **54**, 2651–2653 (1989).
- <sup>17</sup>N. A. Burnham, D. D. Dominguez, R. L. Mowery, and R. J. Colton, *Phys. Rev. Lett.* **64**(16), 1931–1934 (1990).
- <sup>18</sup>G. S. Blackman, C. M. Mate, and M. R. Philpott, *Phys. Rev. Lett.* **65**(18), 2270–2273 (1990).
- <sup>19</sup>B. Saha, A. Peschot, B. Osoba, C. Ko, L. Rubin, T.-J. K. Liu, and J. Wu, *APL Mater.* **5**(3), 036103 (2017).
- <sup>20</sup>T. Jiang and Y. Zhu, *Nanoscale* **7**, 10760–10766 (2015).
- <sup>21</sup>V. M. Muller, B. V. Derjaguin, and Yu. P. Toporov, *Colloids and Surfaces* **7**(3), 251–259 (1983).
- <sup>22</sup>C. Qian, A. Peschot, I. Chen, Y. Chen, N. Xu, and T. K. Liu, *IEEE Elec. Dev. Lett.* **36**(8), 862–864 (2015).